

PAPER • OPEN ACCESS

Threshold Determination Using Bi-hazard Fragility Curves for the Evaluation of Structural Health Monitoring of USHER Technology

To cite this article: M B Baylon *et al* 2020 *IOP Conf. Ser.: Mater. Sci. Eng.* **739** 012002

View the [article online](#) for updates and enhancements.

Threshold Determination Using Bi-hazard Fragility Curves for the Evaluation of Structural Health Monitoring of USHER Technology

M B Baylon¹, F A A Uy², K M S Montes³, K A D Embalzado³

¹Senior Structural Health Engineer, USHER Technologies, Mapua University, Intramuros, Manila, Philippines

²Dean, School of Civil Engineering, Geosciences, Environmental Engineering, Mapua University, Intramuros, Manila, Philippines

³Senior Science Research Specialist 1, PHILSIMS, Mapua University, Intramuros, Manila, Philippines

embylon@usher.ph

Abstract. Structural Health Monitoring (SHM) is not new in the field of structural engineering and its application goes from the monitoring to evaluation of bridges, dams, buildings, and other similar structures. As per National Structural Code of the Philippines (NSCP) Volume 1[1-4], the Implementing Rules of earthquake recording instrumentation of buildings has been continually advancing, but not in the case of bridges and dams. The objective of this paper is to apply the established sensor-driven accelerometer developed by USHER (Universal Structural Health Evaluation and Recording) system in the evaluation of Padre Jacinto Zamora Bridge in Manila; specifically, to determine the proper installation of the developed accelerometer in the identified critical parts of the bridge. SHM addresses the problem of structural integrity assessment and help in assuring repair cost to a minimal. SHM helps quantify the strength of a structure by identifying the damage. Often evaluations are made using visual inspection and by age consideration. Most of the time, the use of this type of evaluation tend to be expensive. Repairs are not directed to the damaged component alone but the whole structure. Hence, the expenditure expands. SHM with the application of Micro-Electro-Mechanical Sensors (MEMS) will allow gathering of data that can be converted in the form of the structure's modal properties (i.e. natural frequency, mode shape, and damping ratio) [6, 7]. Structural health is then determined and be ready to compare it to the structural model simulation results. A method was developed to incorporate seismic fragility curves [5] to determine the thresholds for the evaluation of the structural health. Capacity spectrum method was utilized to derive the seismic fragility function. A Monte Carlo Simulation was used to derive the flood fragility curves.

1. Introduction

In recent times, seismic forces for engineers are inevitable in their designs, especially that of infrastructures. Structural response is utmost important to the structural engineer when he is dealing



Content from this work may be used under the terms of the [Creative Commons Attribution 3.0 licence](https://creativecommons.org/licenses/by/3.0/). Any further distribution of this work must maintain attribution to the author(s) and the title of the work, journal citation and DOI.

with the earthquake hazard. In today's practice of structural engineering, data from previous earthquake event's structural response especially that of bridges are crucial in understanding the principle of performance based design (PBD) of structures. These data can be captured through recording these structural responses, e.g., displacement, velocity, and acceleration, by the system known as structural health monitoring (SHM); thus, paving the way for building instrumentation.

The Padre Jacinto Zamora Bridge is an existing concrete bridge with American Association of State Highway and Transportation Officials (AASHTO) Type IV Girders. The bridge is a reinforced concrete bridge built in the 1960's and became operational in the year 1963. Its length is about 410 meters, linking Pandacan and Paco, Manila.

The objective of this paper is to evaluate the Padre Jacinto Zamora Bridge using USHER technology. Specifically, to determine the proper installation of the developed accelerometer in the identified critical parts of the bridge and to utilize Capacity Spectrum Method (CSM) and Monte Carlo Simulation (MCS) to construct seismic fragility curves and flood fragility curves, respectively, which in turn can be used in the threshold determination for the structural health monitoring of Padre Jacinto Zamora Bridge.

2. Methodology

It can be seen in figure 1 the methodology used for this paper. Using the plans obtained from Department of Public Works and Highways (DPWH) of the Padre Jacinto Zamora Bridge, a structural model was constructed using CSiBridge software application. The structural model was used in the simulation and the installation of sensors. For the simulation, Capacity Spectrum Method was utilized in determining the performance point for each peak ground acceleration (PGA) of the capacity of the critical bridge pier. The performance point, particularly the displacement was compared to the damage levels set by Moschonas et. al. [8] in order to construct the table for the Probability of Exceedance. Using regression analysis to determine the statistical parameters of fragility function, the plot of seismic fragility curves was derived using Matlab. At a 10% probability of exceedance as per Structural Engineers Association Of California (SEAOC), the threshold values were determined at moderate and extensive damage level only. For the installation of USHER, the device was located and installed at approximately the center of mass of the floor plan, but to some extent such as accessibility and internet connectivity (wi-fi access), the device was located strategically [7]. While the device was installed and recording data, the bridge response was being archived and transmitted to the USHER portal and it is ready to download as per the certified structural engineer need for interpretation through a log-in access. The bridge response measured by USHER is then compared to the threshold derived from fragility curves; thus, the bridge is evaluated.

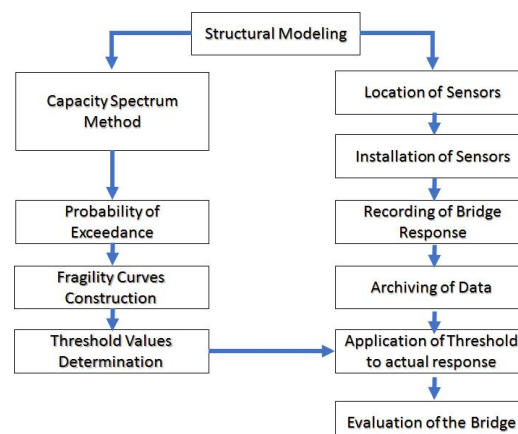


Figure 1. Methodology.

3. Results and Discussions

3.1. Modeling

The model of the bridge is shown in figure 2. In figure 3, the components of the bridge model can be seen.

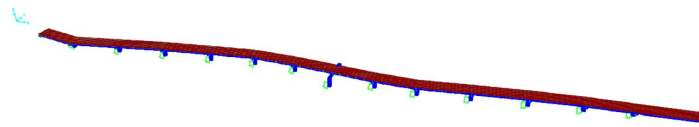


Figure 2. Structural model of Father Jacinto Zamora Bridge.

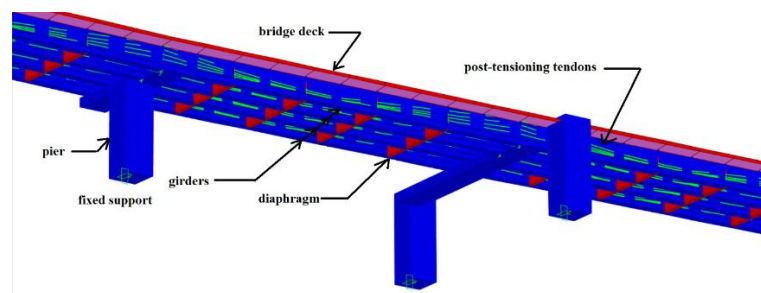


Figure 3. Some of the components of the bridge model.

3.2. Pushover Curves

The pushover curves for the three directions, X-direction, Y-direction, and Z-direction, are shown in figure 4, figure 5, and figure 6, respectively. The nonlinearity of the pushover curve declares the inelastic performance of the bridge. Thus, only the pushover curve in the Y-direction is considered for the capacity curve. Using the CSiBridge, the yield and maximum displacements were determined and it can be seen in table 1. At a base shear of 10.5 MN, the bridge pier yielded at a displacement of 60 mm, whilst at 13.7 MN, it yielded 124 mm. With these displacements, yielded (d_y) and maximum (d_u), and substituting these values using the formulas in table 2 for the respective damage states, the damage limits (lower and upper) can be determined.

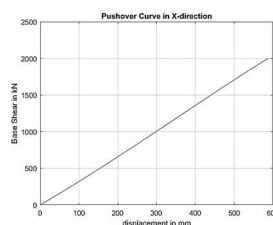


Figure 4. Pushover curve in X-direction.

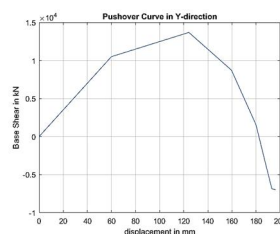


Figure 5. Pushover curve in Y-direction.

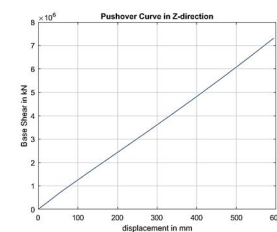


Figure 6. Pushover curve in Z-direction.

Table 1. Pushover curve of the bridge in Y-direction showing the yield and maximum displacements.

<i>Displacement</i>		
<i>(m)</i>	<i>Shear (kN)</i>	
0	0	
0.060	10,494.960	← yield
0.124	13,678.412	← maximum
0.160	8,713.096	
0.180	1,571.146	
0.193	-6,860.886	
0.196	-7,001.300	

Table 2. Damage state limits as per [8] page 446.

<i>Damage State</i>		<i>Required Interventions</i>	<i>limits</i>	<i>Lower limit</i>	<i>Upper limit</i>
D	None	Do nothing	$\leq 0.7 d_y$	0	0.041969
C	Minor/Slight	Inspect, adjust, patch	$> 0.7 d_y$	0.041969	0.081376
B	Moderate	Repair components	$> \min \{ 1.5 d_y, (1/3)*(d_u - d_y) \}$	0.081376	0.102796
A	Major/Extensive	Rebuild components	$> \min \{ 3 d_y, (2/3)*(d_u - d_y) \}$	0.102796	0.124216
As	Complete	Rebuild bridge	$> d_u$	0.124216	∞

3.3. Capacity Spectrum Method

In table 3, the result of the performance point is shown from the simulation of the bridge using CSiBridge's feature of Capacity-Spectrum curve. In structural reliability, the performance function can be derived from the two functions: resistance and the load effect. In this paper, capacity curve is the resistance function, whilst that of response spectrum, it's the load effect. In CSM, this can be captured through the performance points. To illustrate this, one ground motion data was scaled from 0.1g to 2.0g and using an earthquake engineering software application, PRISM, these ground motion data can be transformed to response spectra. The capacity curve, which was derived from pushover curve, can be superimposed to the response spectra. This can be shown in figure 8.

Table 3. A sample tabulation of performance point summary for CSM.
Based on March 3, 2006 Mindoro Earthquake.

<i>PGA in g</i>	<i>X-direction</i>		<i>Y-direction</i>		<i>Z-direction</i>	
	<i>V (kN)</i>	<i>D (m)</i>	<i>V (kN)</i>	<i>D (m)</i>	<i>V (kN)</i>	<i>D (m)</i>
0.2	8.799	0.05	10.325	0.059	7.622	0.444
0.4	17.598	0.101	20.651	0.118	22.865	0.131
0.6	35.196	0.201	41.301	0.236	30.486	0.174
0.8	43.994	0.251	51.627	0.295	45.73	0.261
1.0	52.793	0.302	61.952	0.354	53.351	0.305
1.2	61.592	0.352	72.277	0.413	60.973	0.348
1.4	70.391	0.402	82.602	0.472	76.216	0.435
1.6	87.989	0.503	103.253	0.59	83.837	0.479
1.8	96.788	0.553	113.578	0.649	91.459	0.522
2.0	105.598	0.603	123.903	0.708	106.702	0.610

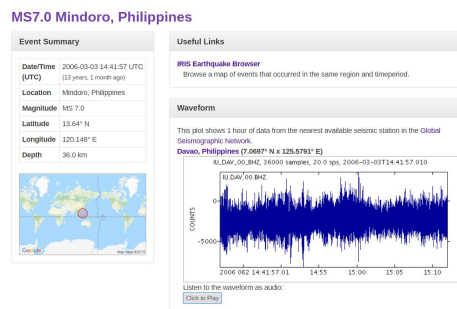


Figure 7. Pertinent data of the ground motion data used in table 3.
(Source: <http://ds.iris.edu/ds/nodes/dmc/tools/event/2192624>)

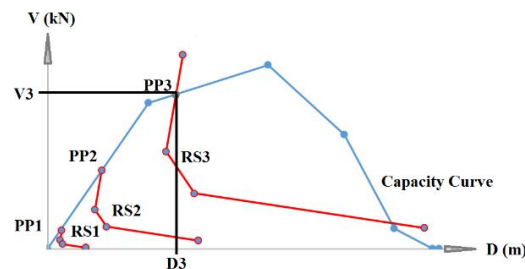


Figure 8. Illustration of the collated performance points from table 3.

All the data from different ground motion data in time history form, were collated and only the Y-direction was considered. In table 4, it summarizes the frequency for each damage state, given the peak ground acceleration (PGA) in g. From this table, the probability of occurrence can be derived as it can be seen in figure 9. It shows the occurrence of damage state present for every PGA. It can be observed that a PGA of 0.5g, the bridge has already reached the complete damage.

Table 4. Basis of the Probability of Occurrence thru frequency for each damage state in a given PGA value.

PGA in g	Damage States				
	D	C	B	A	As
0	12	0	0	0	0
0.1	2	6	0	1	3
0.2	2	3	1	1	15
0.3	0	0	1	1	10
0.4	0	0	1	1	20
0.5	0	0	0	0	12
0.6	0	0	0	0	22
0.7	0	0	0	0	12
0.8	0	0	0	0	22
0.9	0	0	0	0	12
1	0	0	0	0	22

PGA in g	Damage States				
	D	C	B	A	As
1.1	0	0	0	0	12
1.2	0	0	0	0	22
1.3	0	0	0	0	12
1.4	0	0	0	0	22
1.5	0	0	0	0	12
1.6	0	0	0	0	22
1.7	0	0	0	0	12
1.8	0	0	0	0	22
1.9	0	0	0	0	12
2	0	0	0	0	22

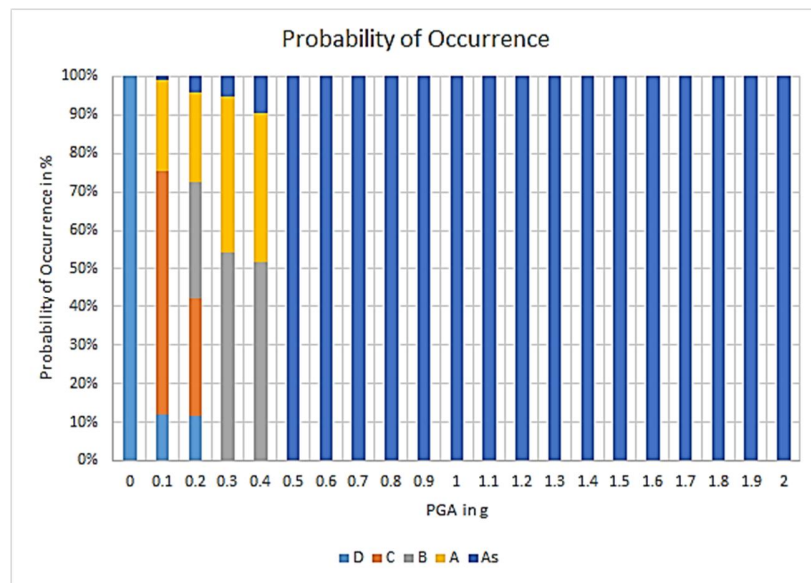


Figure 9. Column chart representation of Probability of Occurrence.

The damage ratio can then be derived from the probability of occurrence by accumulating the probability as it increases in the PGA value, as it can be shown in table 5. This damage ratio values are used as scatter points in the plot of seismic fragility curves. By plotting the natural logarithm of PGA vs. damage ratio, linear regression parameters can be determined graphically. These parameters can now be used as statistical parameters, that is, mean and standard deviation, for the lognormal function nature of the fragility curves, as in equation (1). The seismic fragility curves are then plotted using Matlab, as shown in figure 10, 11, 12, 13, and 14. The values of these fragility curves are listed in table 6. Based on the derived fragility curves, the focus in determining the threshold values for the structural health monitoring is in the Moderate damage level.

$$Pr = \Phi \left[\frac{\ln(PGA) - \lambda}{\xi} \right] \quad (1)$$

Based on figure 12, the peak ground acceleration that has a probability of exceedance of 10% as per SEAOC provision, is approximately at 0.10g. It means that the bridge is deemed repairable through the bridge components which needs monitoring in the component level. The information earthquake that struck Padre Jacinto Zamora Bridge in April 8, 2017, is shown in figure 15. The superimposed threshold values where incorporated in the USHER device results, that is, the structural response, as shown in figure 16. Also, in this figure, the USHER device recorded a maximum of 2.0 m/sec velocity and a maximum displacement of 2.0 m in one of the nodes, i.e., Node 3 as per structural model of the Padre Jacinto Zamora Bridge.

Table 5. Damage Ratio.

<i>PGA</i> <i>in g</i>	<i>Damage States</i>				
	<i>D</i>	<i>C</i>	<i>B</i>	<i>A</i>	<i>As</i>
0	0.750	0	0	0	0
0.1	0.875	0.667	0	0.250	0.009
0.2	1	1	0.333	0.500	0.056
0.3	1	1	0.667	0.750	0.088
0.4	1	1	1	1	0.150
0.5	1	1	1	1	0.188
0.6	1	1	1	1	0.256
0.7	1	1	1	1	0.294
0.8	1	1	1	1	0.363
0.9	1	1	1	1	0.400
1	1	1	1	1	0.469
1.1	1	1	1	1	0.506
1.2	1	1	1	1	0.575
1.3	1	1	1	1	0.613
1.4	1	1	1	1	0.681
1.5	1	1	1	1	0.719
1.6	1	1	1	1	0.788
1.7	1	1	1	1	0.825
1.8	1	1	1	1	0.894
1.9	1	1	1	1	0.931
2	1	1	1	1	1

Table 6. Probability of exceedance values using regression analysis.

PGA	D	C	B	A	As
0	0	0	0	0	0
0.1	0.262529	0.349355	0.096104	0.154058	0.034732
0.2	0.791589	0.62023	0.338276	0.372199	0.175831
0.3	0.951411	0.761628	0.540476	0.531654	0.339343
0.4	0.988073	0.841159	0.680726	0.643232	0.481114
0.5	0.996789	0.889217	0.77495	0.72249	0.593761
0.6	0.999052	0.919944	0.838555	0.780114	0.680735
0.7	0.999696	0.940484	0.882145	0.822966	0.747407
0.8	0.999895	0.954713	0.912551	0.855487	0.798606
0.9	0.999961	0.964865	0.934138	0.88061	0.838147
1	0.999985	0.972287	0.949721	0.900324	0.868908
1.1	0.999994	0.977828	0.961143	0.916008	0.893029
1.2	0.999997	0.982041	0.969634	0.928638	0.912095
1.3	0.999999	0.985293	0.976027	0.93892	0.927283
1.4	0.999999	0.987839	0.980899	0.94737	0.939473
1.5	1	0.989856	0.984651	0.954378	0.949326
1.6	1	0.991473	0.987569	0.960234	0.957344
1.7	1	0.99278	0.989859	0.965163	0.96391
1.8	1	0.993848	0.991673	0.969341	0.969319
1.9	1	0.994727	0.993119	0.972901	0.9738
2	1	0.995455	0.994281	0.975954	0.977532

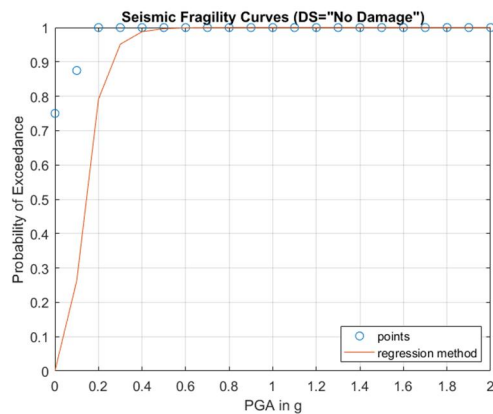


Figure 10. Plot of the seismic fragility curve for damage state of No Damage.

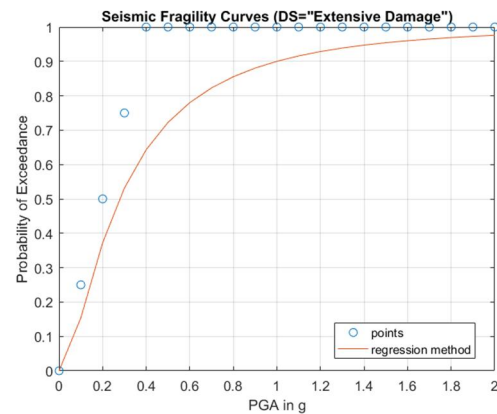


Figure 13. Plot of the seismic fragility curve for damage state of Extensive Damage.

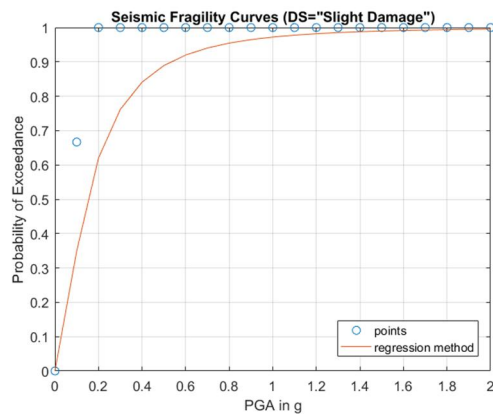


Figure 11. Plot of the seismic fragility curve for damage state of Slight Damage.

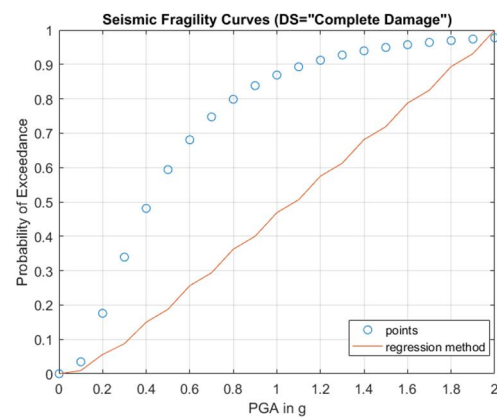


Figure 14. Plot of the seismic fragility curve for damage state of Complete Damage.

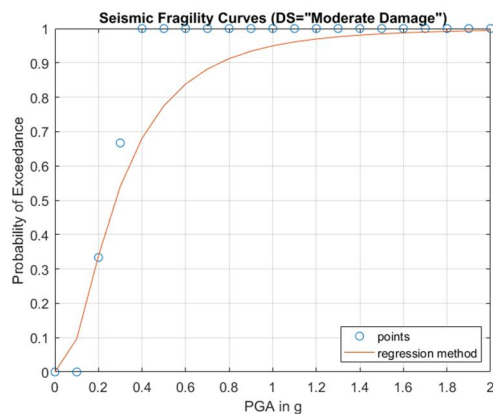
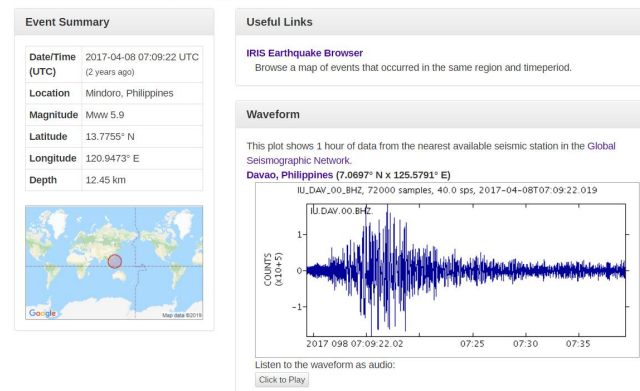
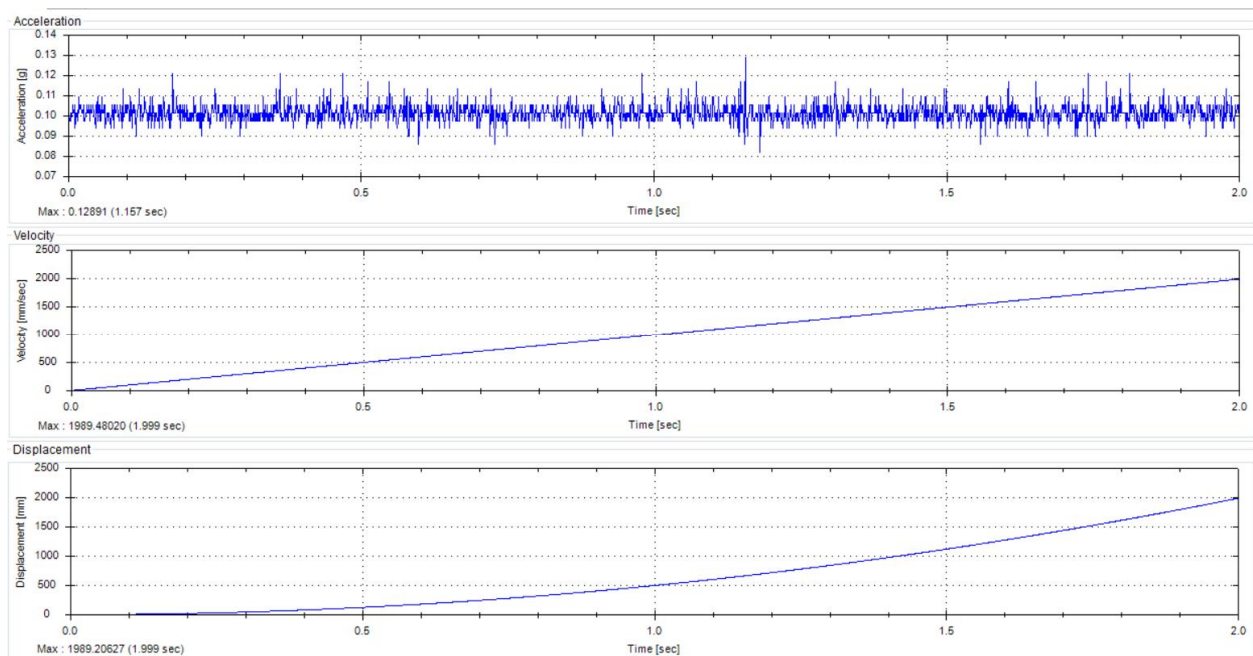
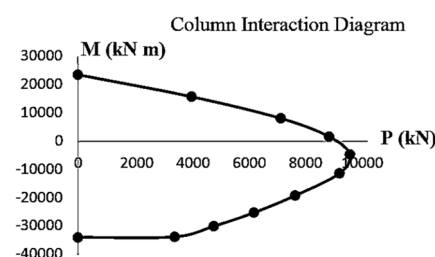


Figure 12. Plot of the seismic fragility curve for damage state of Moderate Damage.

Mww5.9 Mindoro, Philippines**Figure 15.** Information for the ground motion data in April 8, 2017.**Figure 16.** Structural response of the Padre Jacinto Zamora Bridge during the earthquake event last April 8, 2017 as measured by USHER in g, i.e., 0.129g.**3.4. Flood Fragility Curves by Monte Carlo Simulation**

The maximum moment capacity of the columns of the piers are obtained from the column interaction diagram shown in figure 17, which can be acquired from the bridge model. This maximum moment capacity will be used in determining the damage state experienced by the columns once heavy flooding occurs.

**Figure 17.** Column interaction diagram of the critical pier of Padre Jacinto Zamora Bridge.

The Padre Jacinto Zamora Bridge is built across the Pasig River, thus a model of the river was created using a simulation program to obtain its velocity. There were few methodologies used in the previous studies to acquire the water pressure. In the study of Kim et al. [9], the American Association of State Highway and Transportation Officials (AASHTO) and Korean Highway Bridge Design Specification (KHBDS) presented an equation for estimating the water pressure expressed in equation (2).

The damage state is a ratio of the maximum moment demand and the maximum moment capacity. Since the maximum moment capacity is already acquired from the diagram, the maximum moment demand should be identified as well. To get the maximum moment demand, the researchers established a 0 to 100 m/s range to see at what velocity will the bridge experience a collapse damage state. The water velocity is first converted into water pressure using equation (2) from the American Association of State Highway and Transportation Officials (AASHTO) and Korean Highway Bridge Design Specification (KHBDS). The water pressure takes into account the factor for the accumulated debris. Also, the pressure is multiplied to the diameter of the column to get the distributed load which will be used in the equation (3) and equation (4). The distributed load is shown in figure 18.

$$p = 5.14 \times 10^{-4} C_D V^2 \quad (2)$$

where v is the water velocity and C_D is the drag coefficient which can be determined in table 7. In this study, two failure modes are considered: (1) lack of displacement ductility at bridge piers, and (2) pier failure.

Table 7. Drag coefficient of AASHTO and KHBDS.

Pier Type	C_D
Semicircular-nosed pier	0.7
Square-ended pier	1.4
Debris lodged against the pier	1.4
Wedged-nosed pier with nose angle 90°	0.8

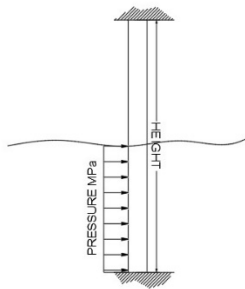


Figure 18. Water pressure transformed into distributed load applied to the fixed-end column.

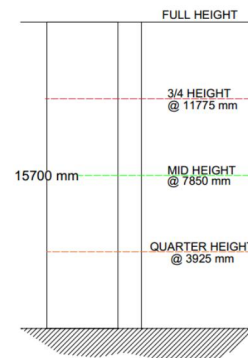


Figure 19. The flood depth classifications used in the study with their corresponding height.

The distributed load, w , will be used in the following equations to get the moment demand at the fixed ends of the column. Equation (3) and equation (4) are expressed as:

$$M_1 = \frac{wa^3(4L - 3a)}{12L^2} \quad (3)$$

$$M_2 = \frac{wa^2(6L^2 - 8aL + 3a^2)}{12L^2} \quad (4)$$

where a is the flood depth, and is the height of the column of the pier. M_1 is the moment at the top end of the column while M_2 is the moment at the bottom end. Since there are two moment demand obtained (M_1 and M_2), the greater moment will be considered as the maximum moment demand. This maximum moment demand, however, varies depending on the flood depth. In the analysis, the researchers classify the flood depth according to the height of the columns. The flood depth is divided into four classifications: (1) at quarter height, (2) at mid height, (3) at $\frac{3}{4}$ of the total height, and (4) at the full height of the column. See figure 19.

In figure 20, it is evident that the columns of Piers 1 and 2 have the same height and that the columns of Pier 3 have a shorter height. The height of the columns of Piers 1 and 2 is 15.7 meters while the columns of Pier 3 are 12.8 meters high.

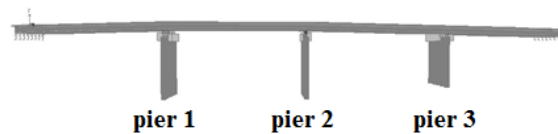


Figure 20. Side elevation of the bridge model, emphasizing the height of the columns.

Since the columns have symmetrical cross-sections, only one column of the pier will be analyzed in the study. The height of that column is 15.7 meters since it is the tallest among all the columns. The analysis was conducted on four flood depth classifications, but the actual flood depths used in the computation are the mean depths, \bar{x} , shown in figure 21. The 20% coefficient of variance was accounted in the analysis.

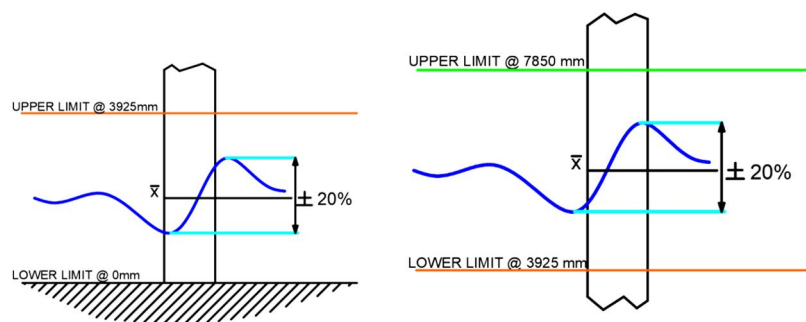


Figure 21. The mean depths at mid height and at quarter height.

Using MS Excel, 1,000 iterations were done per velocity (the 0-100m/s range) and, in those iterations, there are several trials that exhibited results wherein the moment demand exceeded the moment capacity of the column. This exceedance is the probability of failure. The equation for the probability of failure, P_f , is expressed in equation (5).

$$P_F = \frac{\Sigma n}{N} \quad (5)$$

Where N is the number of iterations and Σn is the total number of trials wherein the demand exceeded the capacity. Once the maximum moment capacity, M_c , and the maximum moment demand, M_d , are established, the damage ratio, M_D , can be obtained using equation (6).

$$M_D = \frac{M_d}{M_c} \quad (6)$$

Based on the ductility demand parameters of Dong, Frangopol, and Saydam (2013) presented in table 8, the damage state of the column per velocity is determined.

Table 8. Damage States and Ductility Demand (Dong et al., 2013).

Damage State	Ductility Demand
Minor Damage	$1 \leq MD \leq 2.9$
Moderate Damage	$2.9 \leq MD \leq 4.6$
Major Damage	$4.6 \leq MD \leq 5.0$
Collapse	$MD > 5.0$

The mean and standard deviations needed to generate the flood fragility curves are obtained once all the statistical computations are done in MS Excel. These mean and standard deviations are imported into MATLAB to generate the four flood fragility curves for each flood depth classification.

In figure 22, the bridge has a 10% probability of experiencing “Moderate Damage” at a velocity of 18 m/s when the flood depth is at full height; a velocity of 16 m/s when the flood depth is at mid height; and a velocity of 17 m/s when the it is at $\frac{3}{4}$ of the total height.

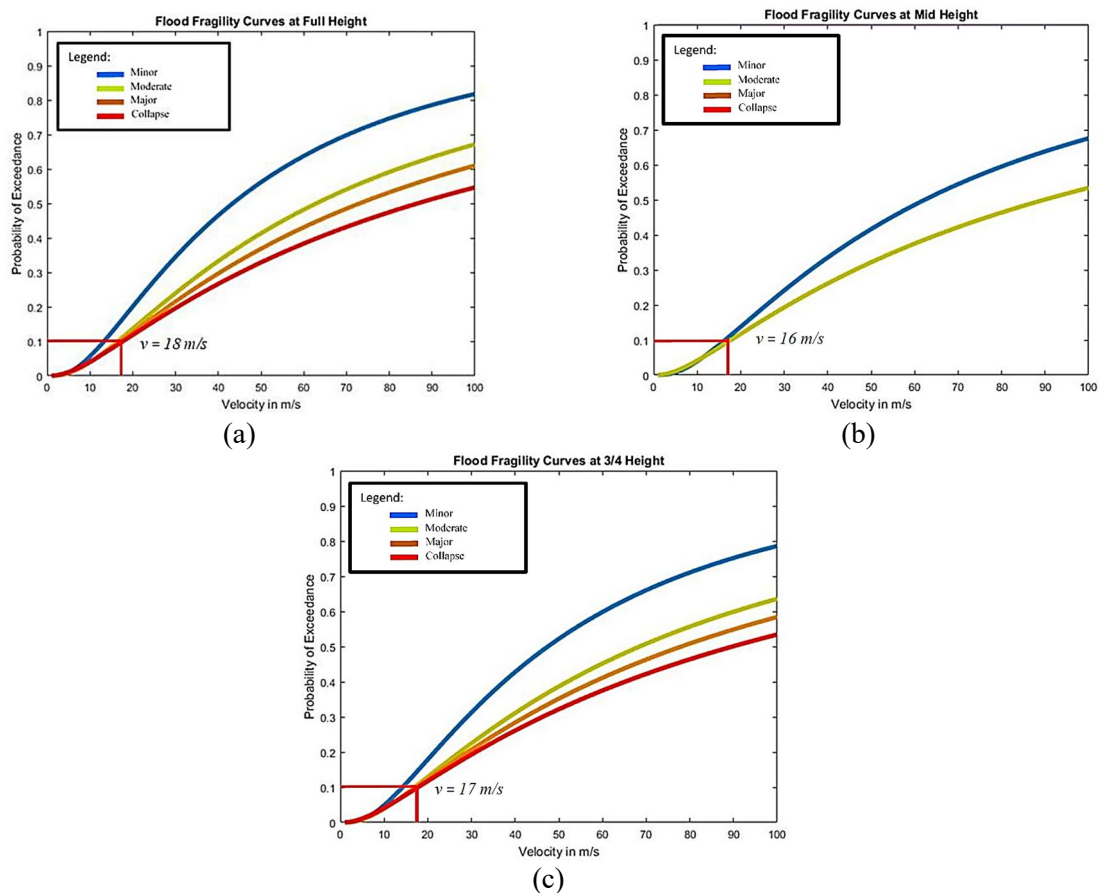


Figure 22. Flood fragility curves of Padre Jacinto Zamora at different flood depth classification.

As you can see, there is no fragility curve when the flood depth is at quarter height of the column because, within the 1,000 iterations, there were no instances that the demand exceeded the capacity. To say the least, the results generated in the iterations tell us that there is “No Damage” experienced by the bridge within the 0-100 m/s range.

4. Conclusion

Based on the findings, the threshold value for a moderate damage to Padre Jacinto Zamora Bridge is approximately at 10% of gravitational acceleration. This threshold value was surpassed by the

maximum response of the structure of 0.129g when the earthquake event happened last April 8, 2017 with a magnitude of 5.9, as recorded by the Universal Structural Health Evaluation and Recording device. Hence, a thorough investigation must be done in the component level of the bridge. In terms of the flood fragility curves, at a 10% of probability of exceedance, the bridge is expected to perform in moderate damage at 18 m/s, 16 m/s, and 17 m/s at a full-height, mid-height, and 3/4 – height of the column pier flood depth.

Acknowledgments

The authors acknowledge Mapua University, Department of Public Works and Highways, Department of Science and Technology for the funding of the research where this paper is based on.

Reference

- [1] Association of Structural Engineers of the Philippines. (1992) National Structural Code of the Philippines, Volume 1. Association of Structural Engineers of the Philippines (ASEP), Manila.
- [2] Association of Structural Engineers of the Philippines. (2001) National Structural Code of the Philippines, Volume 1. Association of Structural Engineers of the Philippines (ASEP), Manila.
- [3] Association of Structural Engineers of the Philippines. (2010) National Structural Code of the Philippines, Volume 1. Association of Structural Engineers of the Philippines (ASEP), Manila.
- [4] Association of Structural Engineers of the Philippines. (2015) National Structural Code of the Philippines, Volume 1. Association of Structural Engineers of the Philippines (ASEP), Manila.
- [5] Baylon M B 2017 *Developing fragility curves in seismic assessment of pier*. LAP Lambert Academic Publishing: Berlin, Germany.
- [6] Dong Y, Frangopol D M, Saydam D 2014 Pre-Earthquake Multi-Objective Probabilistic Retrofit Optimization of Bridge Networks Based on Sustainability, *J. Bridge Eng.* **19**(6).
- [7] Gaviña J R, Uy F A, Carreon J P D 2017 Wireless Smart Sensor Network System Using SmartBridge Sensor Nodes for Structural Health Monitoring of Existing Concrete Bridges, *IOP Conf. Series Mater. Sci. Eng.* **216**.
- [8] Moschonas I F, Kappos A J, Panetsos P, Papadopoulos V, Makarios T, Thanopoulos P 2009 Seismic fragility curves for greek bridges: methodology and case studies, *Bull. Earthquake Eng.* **7** 439-68.
- [9] Kim H, Sim S-H, Lee J, Lee Y-J, Kim J-M 2017 Flood fragility analysis for bridges with multiple failure modes, *Advances in Mechanical Engineering* **9** (3) <https://doi.org/10.1177/1687814017696415>